Makerere University Journal of Agricultural and Environmental Sciences
Vol. 10 (1). pp. 1 - 21, 2021

ISSN 1563-3721

Application of scripting cartographic methods to geophysical mapping and seismicity in Rwenzori mountains and Albertine Graben, Uganda

Lemenkova, P.[1]

[1]Schmidt Institute of Physics of the Earth, Russian Academy of Sciences, Department of Natural Disasters, Anthropogenic Hazards and Seismicity of the Earth, Laboratory of Regional Geophysics and Natural Disasters, (Nr. 303), Bolshaya Gruzinskaya St, 10, Bld. 1, Moscow, 123995, Russian Federation

Corresponding author: pauline.lemenkova@gmail.com

Abstract

Uganda is traversed by the East African Rift System (EARS), which controls its topography and induces high seismicity in the southwestern and western parts of the country, around the Rwenzori Mountains and Albertine Graben. This paper explores the complexity of the geophysical, topographic and geomorphological settings of Uganda for linking the distribution and magnitude of earthquakes to the controlling factors: geomorphology, topography and geophysics. The methodological workflow for an automated plotting of the topographic, geophysical and seismic data includes the following important codes: 'gmt grdimage ug_relief.nc -Cgeo.cpt -R29/35/-1.5/4.3 -JM6.5i -I+a15+ne0.75 -t50 -Xc -P -K > $ps' for topographic visualisation, 'gmt psxy -R -J quakes_UG.ngdc -Wfaint -i4,3,6,6s0.1 -h3 -Scc -Csteps.cpt -O -K >> $ps' for mapping earthquakes, 'gmt img2grd grav_27.1.img -R29/35.5/-1.5/4.3 -Ggrav_UG.grd -T1 -I1 -E -S0.1 -V' for mapping gravity. The steps of the scripting workflow using 'raster' and 'tmap' libraries of R and a variety of GMT modules includes the following most important codes: 'alt = getData("alt", country = "Uganda", path = tempdir()); slope = terrain(alt, opt = "slope"); aspect = terrain(alt, opt = "aspect"); hill = hillShade(slope, aspect, angle = 40, direction = 270)'. The study uses high-resolution spatial datasets GEBCO, EGM-2008, IRIS, gravity grids and SRTM DEM aimed to undertake thematic mapping of Uganda. Nine new maps have been generated using shell scripts of GMT and R for environmental monitoring. Depth of the earthquakes ranges from 4 to 40 Km with frequency of seismic events near Rwenzori Mountains and Albertine Graben for destructive earthquake is less than about five decades. Earthquake magnitudes varied from 3.7 Richter Magnitude Scale (Lake Edward region) to 6.2 Richter local magnitude

scale (M_L) (Lake Albert region). Lake Kivu region has earthquakes with magnitudes between 3.8-5.3. The region of Lake Albert had the highest magnitudes and frequency of seismic events, compared to Lakes Kivu and Edward. Earthquakes around the Lake Albert reached the highest magnitude at 6.2 M_L. Earthquakes around Lake Victoria reach the maximal level of earthquake magnitude at 5.0 M_L, near Lake George - 5.3 M_L. Earthquakes were mostly recorded in the Albertine Graben of EARS in the Albert, Edward and George lakes and occasionally in Lake Victoria.

Key words: Albertine Graben, cartography, GMT, Rwenzori Mountains

Introduction

One of the most fundamental problems to environmental research is the study of the geomorphology sculpturing of relief of the Earth's surface, where major geological processes take place. In this context, the Great Rift Valley of East Africa Rift System (EARS) presents a unique combination of graben basins forming a complex Afro-Arabian rift system. Uganda, located in the eastern part of the EARS (Fig. 1), is notable for the diverse geomorphology, consisting of volcanic hills, mountains, dense hydrologic network of lakes and river basins. The Albertine Graben is a geologically important region of Uganda and one of the most petroliferous rifts in Africa. With an average of 900 meters a.s.l., the country is framed by the mountain ranges both in its eastern and western borders: the Ruwenzori mountain with the highest mountain peak (Alexandra, 5,094 m) and an extinct shield volcano Mt. Elgon (4,321 m) in the east.

Being located in the tectonically active region of the Western Branch of EARS, the western part of Uganda is seismically active, which is caused by rupture of geological faults of EARS. Geographic consequences of earthquakes includes a variety of negative events: extensive movements of landmasses which can be displaced or disrupted, triggered landslides, reactivated volcanism, intensified debris flows and rockfalls in mountainous areas (Lemenkova, 2020d). Earthquakes significantly affect, not only the structure and relief of the surrounding landscapes, but also cause serious problems in social life through the damage to property and/or losses of human life.

In this regards, the cartographic methods of map visualisation have a key role to play in the issues of geomorphological mapping, because it enables one to effectively assess the topographic variability of the country. However, despite the actuality and challenge of GIS approaches, no research has been done on the application of scripting cartographic methods to geophysical mapping of Uganda; neither has there been much use of programming languages for this purpose. The existing literature presents maps of Uganda with the application of traditional GIS-based applications for

Figure 1. Topographic map of Uganda. Mapping: GMT.

visualisation (Aanyu and Koehn, 2011; Herbert *et al.*, 2014; Call *et al.*, 2017; Guma *et al.*, 2019; Byakagaba *et al.*, 2019). At the same time, scripting cartography enables rapid and accurate mapping using machine learning approach generating computer-based graphics. Machine learning technologies are bringing new opportunities and challenges to cartography, especially to geoinformation processing (Lemenkova, 2020a).

Some regions of Uganda cannot be directly accessed for *in-situ* observations and field mapping, e.g. deeply dissected mountainous ridges, regions with hidden relief exposure or deep weathering, and areas with dense vegetation coverage (Bahiru and Woldai, 2016). This signifies the relevance of the computer-based applications,

such as scripting techniques, in geophysical mapping of Uganda, and the importance of high-resolution open data as raster grids for geophysical data processing.

Therefore, the objective of this paper was to (i) investigate the tectonic factors associated with seismicity in the western region of Uganda located within the EARS; (ii) evaluate the interaction effects of geomorphological setting and geophysical anomaly fields on topographic patterns of the country; and (iii) determine the cartographic feasibility of scripting mapping and applied programming methods for geological-geographical mapping of Uganda.

Regional setting

Uganda is situated within the western branch of the EARS (Fig. 1), which is one of the greatest and most prominent tectonic features of Africa, and a classic example of a continental rift which has attracted attention of the world's reputable geologists (Déprez *et al*., 2013; Rooney, 2020; Ebinger, 2021). The formation of the EARS has been caused by continental extension, fracturing and thinning of the Earth's lithosphere (Chorowicz, 2005). The EARS extends in Africa from the depression of Triple Junction in the Afar Triangle of Ethiopia in the north, then continues in eastern Africa and terminates in Mozambique. The Western branch of the EARS continues as the Albertine Graben, which reflects the complex geodynamic evolution in the Western branch of the East African Rift System (Schneider *et al*., 2016). Lake Albert Rift experienced geologic evolution from large basin to narrow rift (Simon *et al*., 2017).

The Western Branch of the EARS continues from Lake Albert in the north towards Lake Malawi (Nyasa) in the south. This region experienced a sequence of earthquakes within the Western Rift of the EARS, as a result of active deformation in an early-stage rift (Schaff *et al*., 2019). The active tectonic movements are reflected in asymmetric geomorphology of the EARS, which differs in Western and Eastern Branch (Calais *et al*., 2006). Regional elevations of the western branch of the EARS are less expressed compared to its Eastern Branch, although some segments demonstrate the greatest depressions on the Earth. These are expressed in deep rift lakes of Uganda, located in the Albertine Graben: the Albert Lake, the Edwards Lake and the George Lake (Fig. 1). Lake Victoria is located eastwards of the Albertine Graben, also tectonically and geologically connected to the EARS although.

The Rwenzori Mountains present a significant geomorphological element of the SE Uganda. The topography of the Rwenzori Mountains presents steeply incised valleys and glacial landforms (Kaufmann and Romanov, 2012) and consist of an the highest alpine mountain chain in the western branch of the EARS (Bauer *et al*., 2012,

2013). The Rwenzori Mountains are the highest rift mountains on earth with long and narrow separated rifts and occuring volcanism. The length of the separate rift valleys reaches up to 150 Km and width is up to 70 Km (Ring, 2014). Large elevation amplitude reflects the complex geodynamic setting of the Albertine Graben region (Fletcher *et al.*, 2018).

Deep seismicity (depths 0-30 Km) and volcanism of the Albertine Graben in Uganda (Fig. 2) are related to the faults in the lower lithosphere crust (Ebinger, 1989). Riverine

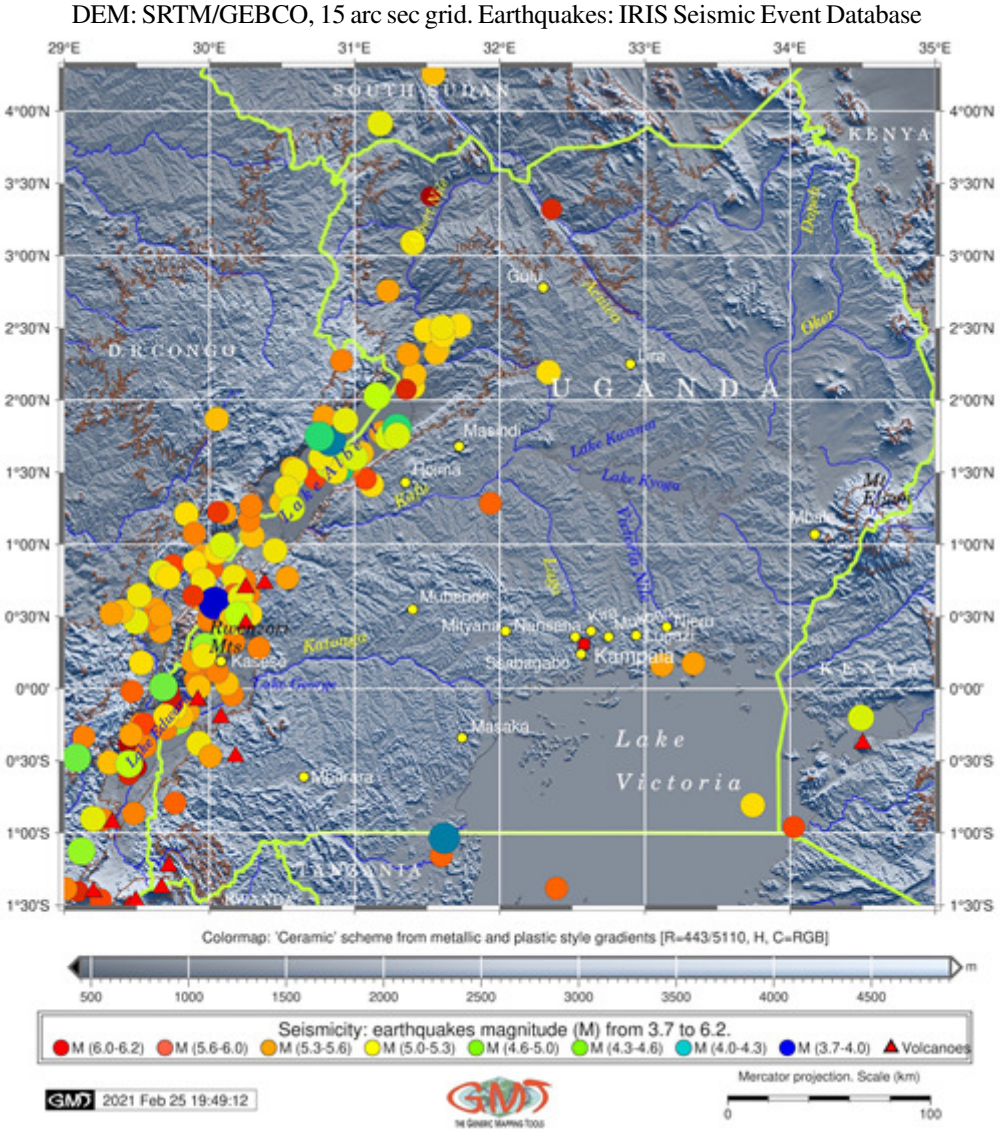

Figure 2. Seismicity in Uganda. Mapping: GMT.

and lacustrine systems of Uganda present a complex hydrological network, which mirrors its regional geologic and geodynamic setting, presenting an important structural element in the geomorphology of Uganda. The basins of lakes are located both in the floor of the valley of the East African Rift, as well as in the depressions amongst the Rwenzori mountains and eastern mountain chains. The correlation between the environmental and geophysical setting of EARS can be illustrated by the hydrological cycle of the lakes which moderately affects earthquake activity. Specifically, seasonal hydrological loading of the EARS lakes generates stress at seismogenic depths which correlates with seismicity rates in the western branch in the EARS (Xue *et al*., 2020).

Materials and methods

Data collection

The datasets were obtained from open sources, processed and inspected in terms of accuracy, reliability and correctness were clipped over Uganda, using first the coordinate extent (29° to 35°E, 1.5°S to 4.3°N) and then the mask for the country using Digital Chart of the World (DCW). The maps for visualising topography and seismicity of Uganda were plotted in Mercator projection for compatibility of graphics. The datasets were taken from the open repositories: (i) General Bathymetric Chart of the Oceans (GEBCO) topographic grid (Schenke, 2016) used in Figure 1 known for unprecedentedly high resolution, precision and reliability compared to other data (Lemenkova, 2020e); (ii) tabular data from IRIS database used in Figure 2; (iii) geoid Earth Gravitational Model EGM-2008 (Pavlis *et al*., 2012) used in Figure 3; and (iv) gravity satellite-derived data from the CryoSat-2 and Jason-1 (Sandwell *et al*., 2014) used in Figures 4 and 5. The Shuttle Radar Topography Mission (SRTM-90) data was used for mapping Figures 6 to 9.

All seismic data were downloaded through the IRIS Web Services (https://ds.iris.edu). The facilities of IRIS Data Services (IRIS Transportable Array, 2003), and specifically the IRIS Data Management Center, were used for access to waveforms, related metadata, and/or derived products used in this study (Albuquerque Seismological Laboratory (ASL)/USGS, 1988). Materials provided by the IRIS Education and Public Outreach Programme have been used in this study for mapping seismicity of Uganda.

The technical details of these data, their resolution, algorithms of generating raster files, source origin, including the satellite specifications and technology of data capture used to produce these datasets are available in the open repositories (GEBCO, IRIS, EGM-2008, SRTM), supported by the descriptive materials. Seismic data for this study uses the 766 earthquake records showing magnitude and location of the earthquakes in around the Rwenzori mountains and neighboring areas in the west of

World geoid image EGM2008 vertical datum 2.5 min resolution

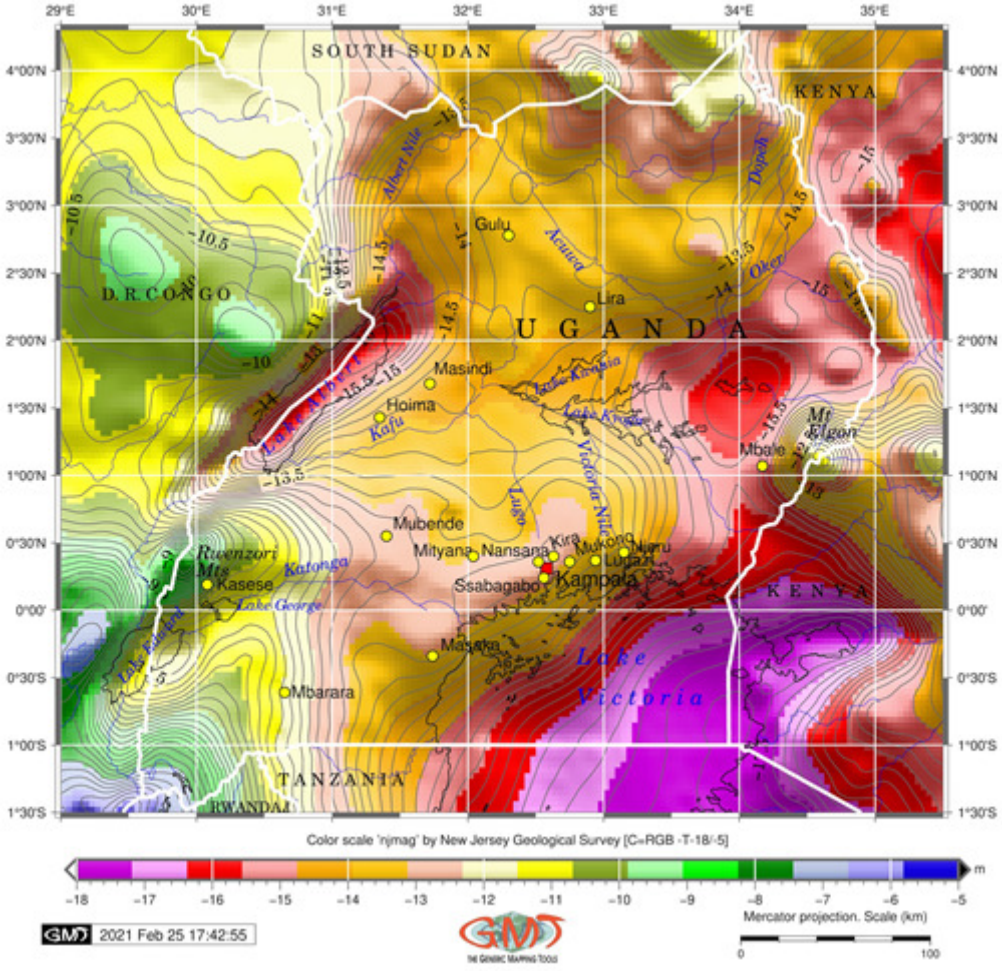

Figure 3. Geoid model of Uganda. Mapping: GMT.

Uganda captured from the IRIS database for the period from 1973 to 2021. This dataset is more compact compared to similar works, e.g. 21,700 local earthquakes with recorded magnitudes •0.5 to 5.1, which helps to visualise the earthquakes events on a map (Batte *et al*., 2014).

The geoid grids were converted using GMT module 'grdconvert' for the GRD format which is readable by the GMT as follows: 'gmt grdconvert s45e00/w001001.adf geoid_TZ.grd'. Other data were processed directly using original NetCDF format. The data were re-projected to the Mercator projection using GMT flag '-JM6.5i'; followed by implementing the data extent: '-R29/35.5/-1.5/4.3' for the maps in Figures 1 – 5 made using GMT.

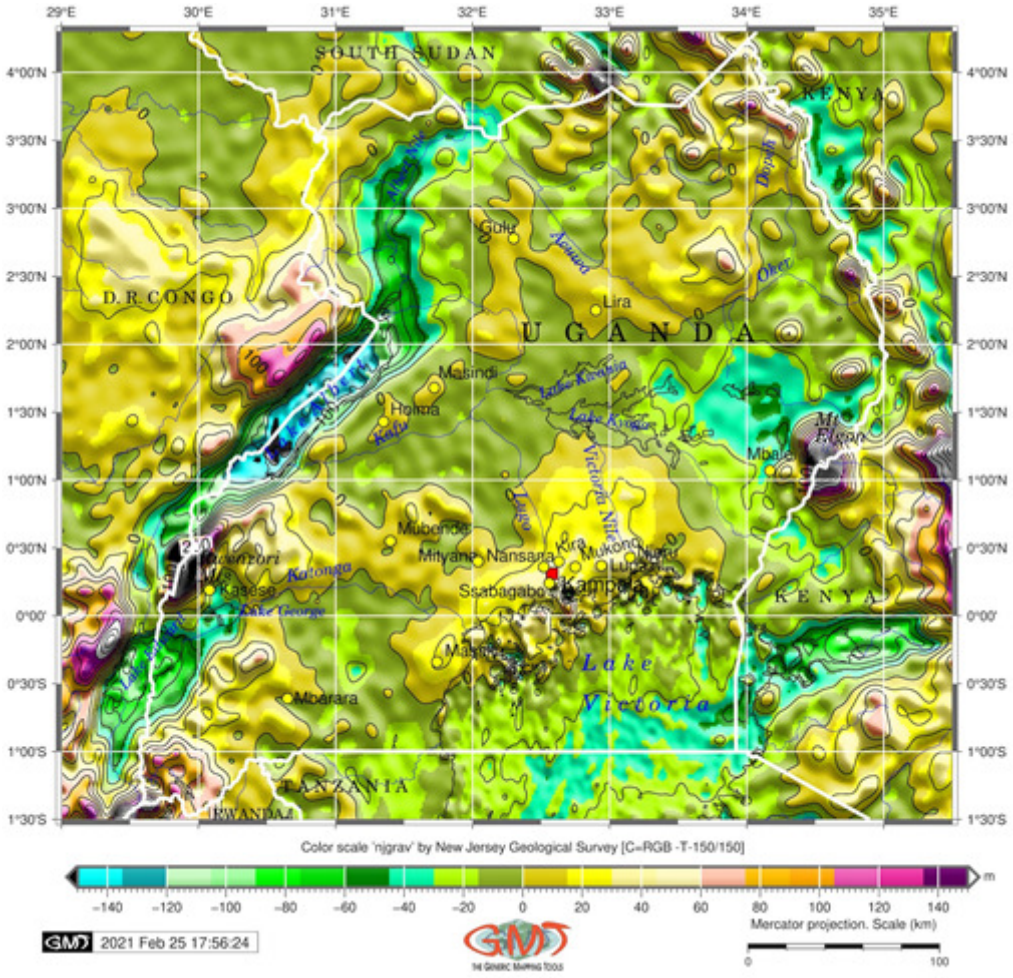

Figure 4. Free-air gravity (Faye's) map of Uganda. Mapping: GMT.

GMT cartographic scripting toolset

Maps in Figures 1–5 were plotted with GMT cartographic scripting toolset (Wessel *et al*., 2019), using a variety of the modules and techniques of scripting described in the existing technical works (Lemenkova, 2020c, 2020d). Figures 1–5 show spatial variations in the topographic, seismic and geophysical setting of Uganda, using visualised high-resolution datasets.

Figure 1 showing spatial variations in topography of Uganda was carried out using the 'grdimage' module of GMT by the following methodological approach: 'gmt grdimage ug_relief.nc -Cgeo.cpt -R29/35/-1.5/4.3 -JM6.5i -I+a15+ne0.75 -t50 -Xc -P -K > $ps'. The isolines were added on top of the visualised raster by 'grdcontour' module: 'gmt grdcontour ug_relief1.nc -R -J -C1000 -

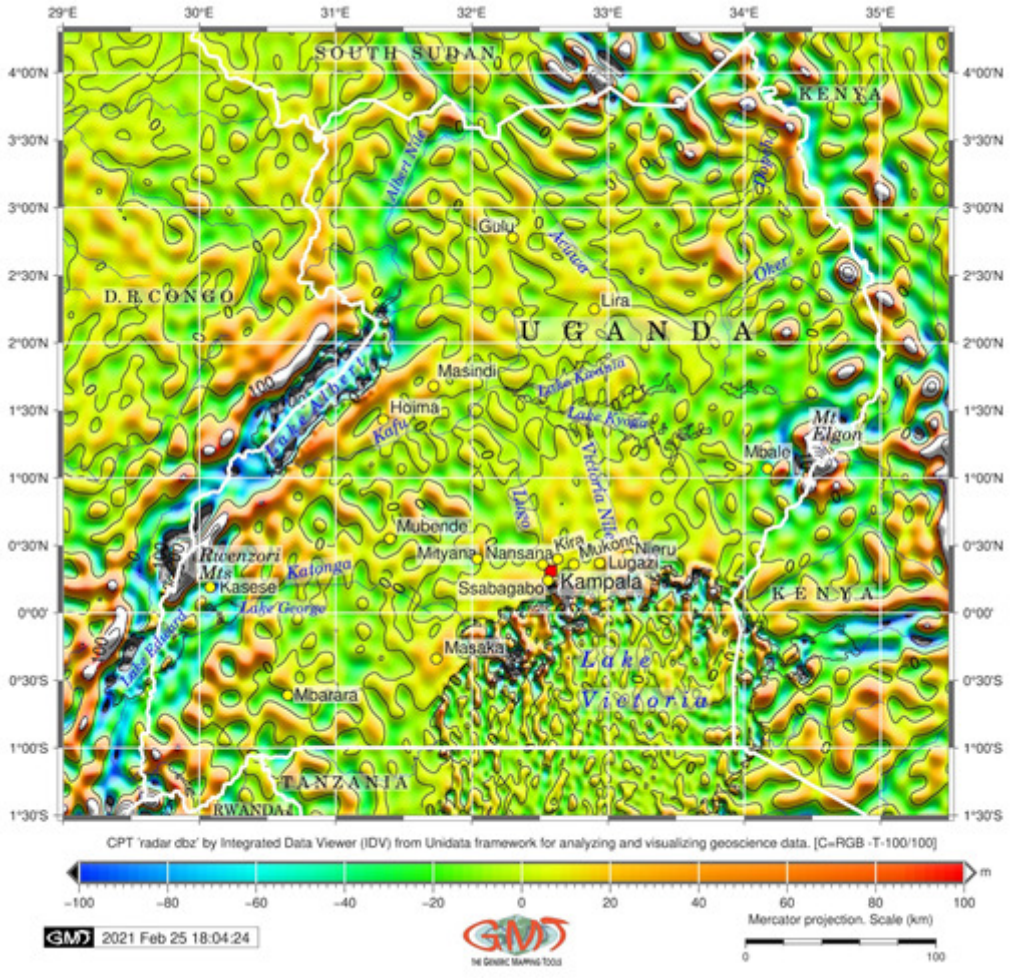

Figure 5. Vertical gravity gradient map of Uganda. Mapping: GMT.

A1000+f7p,26,darkbrown -Wthinner,darkbrown -O -K >> $ps'. The colour palette was extended according to the data range in Uganda as follows: 'gmt makecpt -Cwiki-schwarzwald-cont -V -T443/5110 > pauline.cpt'. The area of the country was clipped using DCW layer in vector formed, which served as a mask for plotting the image over the semi-transparent background with neighbor countries: 'gmt pscoast -R29/35/-1.5/4.3 -JM6.5i -Dh -M -EUG > Uganda.txt'.

Figure 2 shows the seismicity of the Uganda. In total 766 samples of seismic events have been acquired over the Rwenzori Mountains and surroundings in various years (1973-2021) across the EARS in Uganda from the IRIS database. Samples were taken using the IRIS Earthquake Browser and saved initially in the .xls format. Afterwards, the seismic events were identified by the name of the region and by the

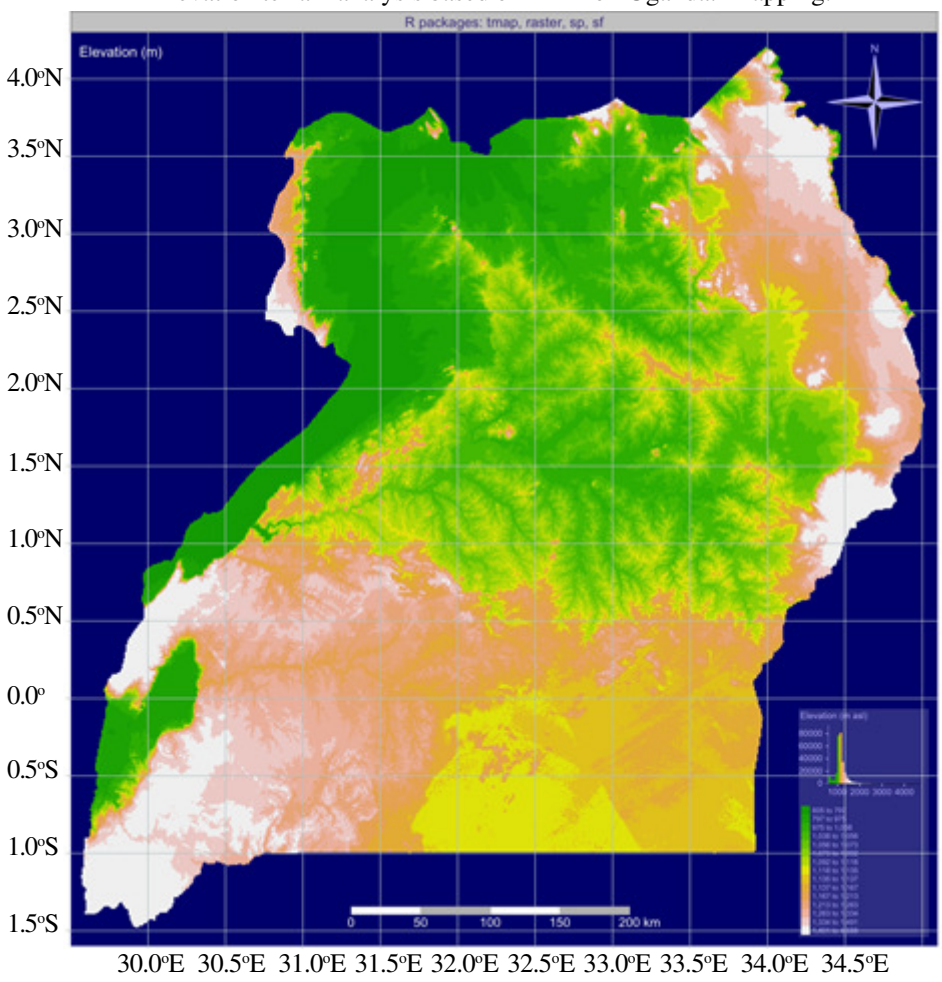

Figure 6. DEM SRTM-90 elevation heights map of Uganda. Mapping: R.

focal depth of event, expressed as in kilometers. Recent earthquakes (2020–2021) were recorded in the following locations: 38 Km WNW of Bundibugyo, 11 Km SSW of Kilembe, 47 Km W of Kigorobya, 16 Km NE of Ntungamo, 26 Km SSE of Kasese. Likewise, the database was inspected for the events started from 1973 and the events were plotted using colour distinction for the magnitude of the events. The samples were visualised using the 'psxy' module: 'gmt psxy -R -J quakes_UG.ngdc -Wfaint -i4,3,6,6s0.1 -h3 -Scc -Csteps.cpt -O -K >> $ps'.

Figure 3 shows the distribution of geoid undulations over the study area; which reflects the deficit of landmasses well illustrating the relationship between the geophysical and geomorphological data. The map has been plotted using the EGM-2008 grid, using the NGA open source which provided raster data complete to spherical harmonic

Slope terrain map based on SRTM-90 DEM of Uganda. Mapping: R

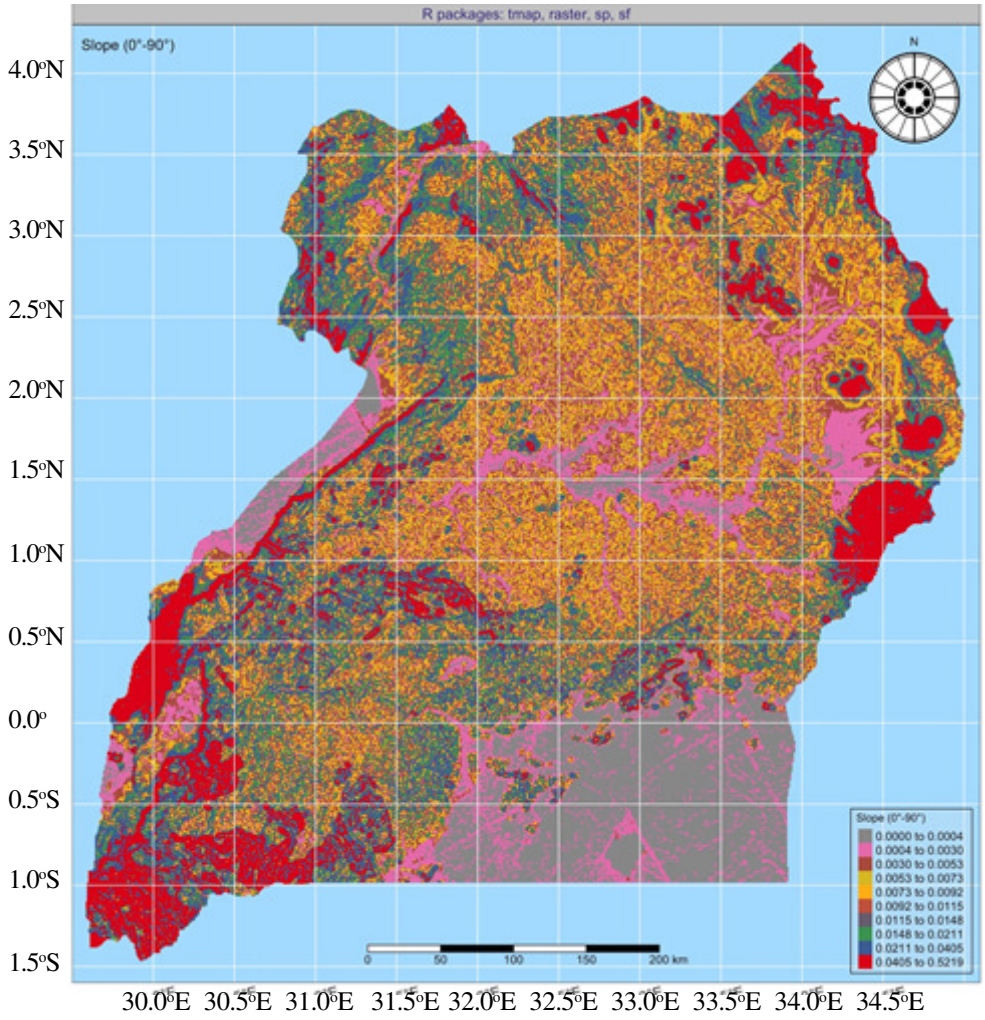

Figure 7. Slope model map of Uganda. Mapping: R.

degree and order 2159, and contains additional coefficients extending to degree 2190 representing gravitation model of the Earth. Differences in the anomalies of the Earth's gravity field are caused by the variations in the mass distribution, which enables to model the shape of geoid.

The data were visualised using the code 'gmt grdimage geoid_UG.grd -Ccolors.cpt -R29/35.5/-1.5/4.3 -JM6.5i -P -Xc -I+a15+ne0.75 -K > $ps' repeated for the neighbor segment. The 'grdcontour' was used for interpolation of the isolines plotted with interval of every 0.25 m: 'gmt grdcontour geoid_TZ.grd -R -J -C0.25 -A0.5+f9p,25,black -Wthinner,dimgray -O -K >> $ps'. The visualising of the raster

Aspect terrain map based on SRTM-90 DEM of Uganda. Mappin: R

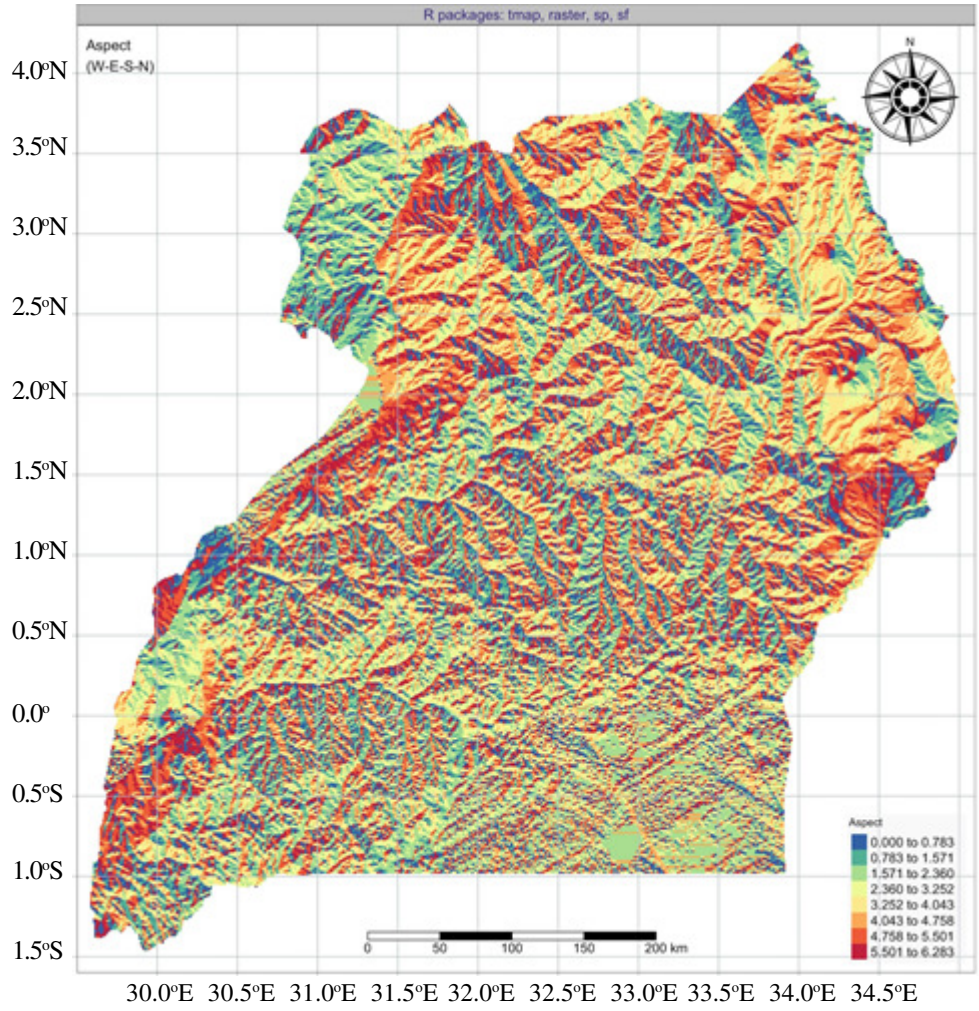

Figure 8. Aspect model map of Uganda. Mapping: R.

image outputs to produce quality maps for enhanced visualisation has been made using the 'psconvert' module: 'gmt psconvert Geoid_UG.ps -A0.5c -E720 -Tj -Z'.

Figures 4 and 5 illustrate the anomalies in the gravity grids. These gravity maps show variations in the structure composition of the Earth's crust, which has an applications in pure and applied geophysics; as well as geological investigations reflecting the Earth's crust density. The data were initially converted into the GRD format as follows: 'gmt img2grd grav_27.1.img -R29/35.5/-1.5/4.3 -Ggrav_UG.grd -T1 -I1 -E -S0.1 -V'. Afterwards, the data extremes were inspected using the Geospatial Data Abstraction Library (GDAL) by the following code: 'gdalinfo grav_UG.grd -stats'.

Hillshade terrain analysis based on DEM of Uganda. Mapping: R

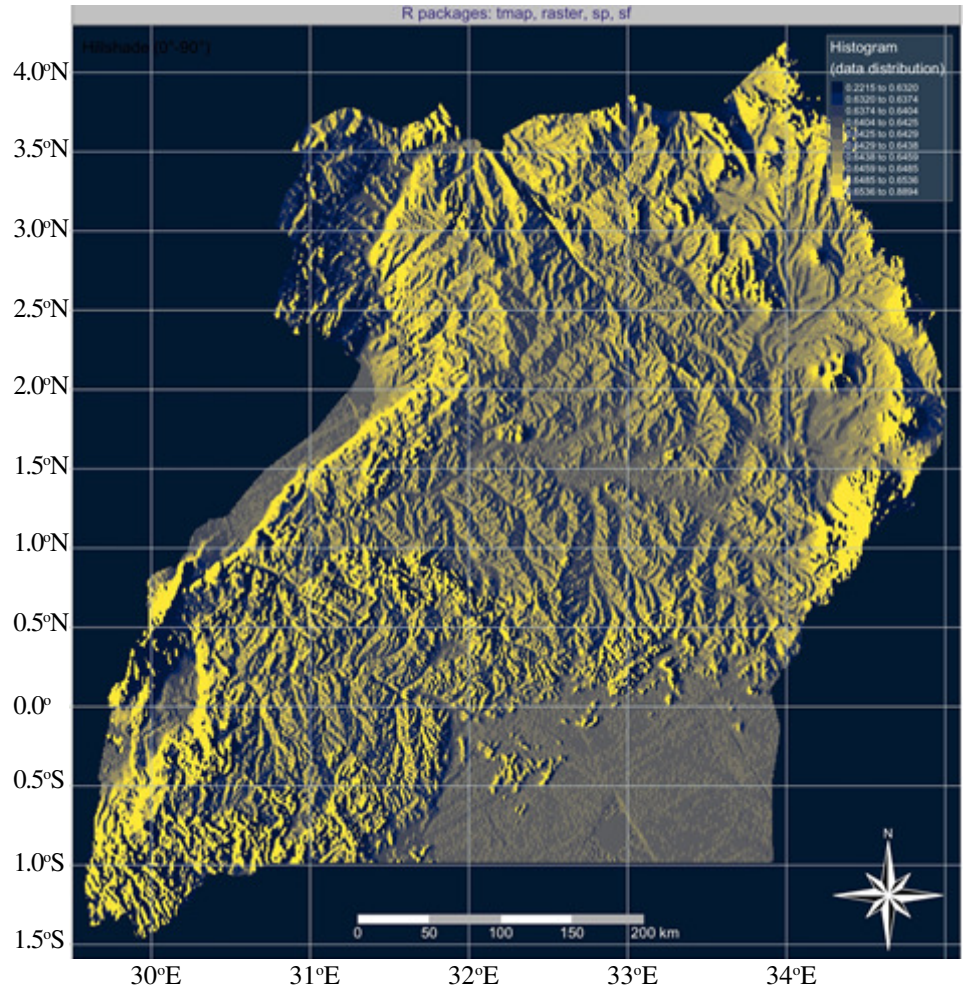

Figure 9. Hillshade visualization map of Uganda. Mapping: R.

Using the obtained values and analysis of the general data extent the colour palette was adjusted to visualise the grid: 'gmt makecpt -Cnjgrav -T-150/150 > colors.cpt'.

Figure 5 illustrates the gravity adjusted for the vertical correction. A gravity anomaly shows the difference between gravity on the geoid and gravity on the reference spheroid. As a complex geophysical value, this was produced by mass distributions that cause the geoid to deviate from the spheroid. Land measurements demonstrated in gravity grid of Figure 5 are made above sea level in Uganda region. Measured gravity (EGM-2008) is reduced to the sea-level. Gravity anomaly is received by subtracting normal gravity on the spheroid. The Earth Gravity Model EGM-2008, a spherical harmonic expansion of the geopotential of the Earth, has been used to map the gravity grid over Uganda.

R software

The SRTM-90 data embedded in R were used in geomorphometric maps (Figs. 6 to 9) for experiments with topographic relief modeling with each maps processed using a combination of 'raster' (Hijmans and van Etten, 2012) and 'tmap' packages (Tennekes, 2012), applying available workflow modified and adjusted to the case of Uganda (Lemenkova, 2020b). The elevation data were downloaded for the whole country using the 'getData' function of 'raster' package: 'alt = getData ("alt", country = "Uganda", path = tempdir())'. The elevations are visualised in Figure 6 using R package 'raster', which shows readable DEM. The derivatives were modeled as slope, aspect and hillshade of the topography of Uganda as shown in Figures 7-9, respectively.

Additional cartographic adjustments included adding embellishments and decorations: north arrow, background colorisation, placing and rotating ticks on the cartographic grid and soon, which were adjusted in 'tmap' package of R. The geomorphometric derivatives of slope (Fig. 7), hillshade (Fig. 9) and aspect (Fig. 8) show the landform features associated with the topography of Uganda. The visualisation of the maps was performed using 'tmap' functionality. Selecting colour palette for each of the maps were done using 'tmaptools::palette_explorer()'; followed by the set up: 'tmap_mode("plot")'. The setup of each of the maps was done using a set of functions of the 'tmap' package that started with generation of the file (here: 'map1') and its layout: map1 <- tmap_style("natural").

Afterwards, every cartographic element was added using lines of code implicitly adjusting its appearance; e.g., general settings for raster were set up using the command: 'tm_raster(title = "Slope (0\u00B0-90\u00B0)", palette = "-Set1", style = "quantile", n = 10, breaks = c(5, 10, 20, 30, 40, 50, 60, 70, 80, 90), legend.show = T, legend.hist = F, legend.hist.z=0)'. Slope modeling was defined using function settings. The same approach was applied for other cartographic elements, placement and position, e.g.: 'tm_compass(type = "radar", position=c("right", "top"), size = 7.0)', which defines compass placement and appearance and 'tm_graticules(ticks = T, lines = T, labels.rot = c(15, 15), col = "white", lwd = 1, labels.size = 1.0)'. The advantage of the presented scripts lies in repeatability of the code applied for all maps prepared using R: (Figs. 6-9).

The feature extraction presented in slope, aspect and hillshade of Uganda has been presented using embedded algorithms of R 'raster' techniques and supported by 'tmap' for finer visualisation. Modeling slope and aspect were made automatically by R, using algorithms developed from theoretical analysis of the DEM SRTM applying, principles of geoscience and computer modeling, embedded mathematical functions, and computer-based data processing. The integration of these functionalities

in R enabled data interpreting, modeling and visualising for mapping the Earth's surface of Uganda using input SRTM-90 DEM data.

Results and discussion

Figure 1 demonstrates the distribution of the topographic patterns over the surface of Uganda. All map elements represent the topographic abstractions of real phenomena of Earth's terrain surface showing the relief of Uganda. Thus, an important step in interpreting this map is to analyse a legend showing the topography of Uganda. In general, there is an increase in topographic values in SW region of the country (1,500 to 2,000 m), reaching the peak in the Rwenzori Mountains with elevations exceeding 5,000 m (coloured dark green in Figure 1), which reflects the geological history of SW Uganda formed under the EARS influence. During the formation of the EARS valley, the area between the Albertine Graben and Lake Victoria was being warped, which is well reflected in Figure 1. Parts of the relief in the SW Uganda were raised; while others lowered as a response to the tectonic deformations and processes of faulting and rising. Such geodynamic processes resulted in the subdivision of the relief in SW Uganda which is more diverse compared to the C and N parts of the region.

Figure 2 shows the distribution of earthquakes in Uganda from 1973 to 2021. Symbols on the map are classified along a continuum, with pictorial representation of the magnitude of earthquakes ranging from 3.7 (blue) to 6.2 (bright red) with gradually changing gradation. The geometric symbols of volcanoes are shown as triangles, mostly concentrated in the EARS in the west of the country. Focal depths of the recorded earthquakes vary from 22.6 to 39.9 Km, that means, all the recorded and visualised earthquakes in Uganda are of shallow focus (between 0 and 70 Km deep). According to Richter scale, the magnitude of earthquakes here ranged from 3.4 to the maximal 6.2, with majority of the events as are moderate (around 5) and only one earthquake was strong (6.2).

Figure 3 shows the geoid model of Uganda based on the EGM-2008 grid. The smallest values of geoid values (-18 to -16 m) are notable over the N part and coasts of Lake Victoria and SE region of the country (purple to magenta colours in Figure 3), which reflects the influence of the geophysical mass distribution including rock density, which depends on regional geological setting. Lake Albert shows values of about -16 m; while the Rwenzori Mountains have higher values (ca. -10 to -8 m, greens in Figure 3). The central plateau of Uganda is covered by values of around -14 m (ochre, Fig. 3). Over the NW parts of the country where topography is lower,

the geoid values are about -12 (light yellow, Fig. 3) which shows the deficit of landmasses reflected in the geophysical characteristics of the terrain.

Figure 4 shows the free-air gravity map of Uganda in Faye's reduction. The highest values of gravity (>130 mGal, dark magenta, Fig. 4) are notable over the mountainous areas. Such examples include the regions around Mt. Elgon and Rwenzori Mts and some small areas in the SW of the country around the border with Rwanda, where values of gravity overstep 110 mGal. Central areas of Lake Victoria have values of -30 to -44 mGal. Central plains are covered generally by values of 0 to -16 mGal (greens in Figure 4). The city agglomeration around Kampala has values 16–30 mGal. The generally uniform pattern of gravity distribution over the central basin areas of the lakes Kwania and Kyoga (0 to -16 mGal) reflects the geophysical anomalies in central Uganda. The decrease of gravity values in Lake Albert basin (<-136 mGal, cyan, Fig. 4) well reflects the depression of the topographic landmass, and vice versa, the higher anomalies correspond to the mountain ranges in Rwenzori and Elgon Mountains in Uganda.

Figure 5 shows the distribution of the values of vertical gravity gradient over the surface of Uganda. In the central plains of Uganda, the values range from less than 30 mGal (orange colours in Figure 5) to over -40 mGal (bright greens in Figure 5). As such, the green colours serve as a link for map readers between markers of lower gravity values (blue colours) and higher values (red colours). In addition to the distribution of gravity grid, the interpretation of this map suggests a decrease in landmasses (which corresponds to the lower gravity values) along the EARS, as an effective connotation of seismic events and associated risk of environmental and agricultural possible danger and distribution of areas prone to risk. The lowest values occur in the SE area of Uganda over the basins of Lakes Albert and Edward (values -60 to -80 mGal) preceded by the smaller Lake George (-45 to -60 mGal). The higher values reflect gravity anomalies that follow the variations in values of the gravitational force over the surface of the Earth which are caused by the abnormal concentrations of landmasses in a certain region. This is the case for the mountain ranges, as visible over the Rwenzori Mountains and Mt. Elgon (values over 100 mGal). Conversely, negative values result from the depression of the landmasses which cause negative gravity anomalies in Uganda: lakes Albert and Edward.

The presented geomorphological models (Figs. 6-9) improve and contribute to general cartographic database on Uganda presenting general geomorphometric parameters: (i) slope, ii) aspect, iii) hillshade and iv) elevation. The geomorphometric maps of Uganda contribute to topographic modeling, support decision making in agricultural monitoring and management using information on the slope steepness and aspect

orientation (WESN) which is useful for plant management. More explicitly, analysis of the geomorphology based using data from morphometric analysis supports the needs of seismicity monitoring in disaster risk prevention. Figure 6 shows DEM SRTM-90 elevation heights map of Uganda. The density and significance of the riverine and lacustrine network in Uganda are well expressed in the visualised DEM in Figure 6, evidenced by the dominating values of heights in C and N Uganda (green colours in Figure 6); while the S and NE regions are covered by mountains. The statistically prevailing values of the topographic elevations in Uganda in comparison with the surrounding areas are illustrated by the histogram of data distribution (Fig. 6).

Figure 7 shows the slope model map of Uganda. Higher values in slope gradient are notable in the mountain slopes of the Rwenzori and Elgon Mountains (bright red, Fig. 7) than over the central part of Uganda (beige and ochre, Fig. 7), as well as basin of lakes (grey to pink color, Fig. 7) which is a result of the variations in topographic elevations with more steep changes in higher mountains. The marks of volcanism and tectonic impacts are detected in the landscapes of the SE Uganda which brought up new gradients to the landscape slopes. Thus, general axis of upward curvature along which the land surface was tectonically uplifted extends to the east of the ESRS valley and Albertine Graben.

Figure 8 shows the aspect model map of Uganda depicting the orientation of the slopes. For example the floor of the EARS valley has generally the S and SE oriented slopes, while the landscapes of the Rwenzori Mountains mostly lie to the opposite S-N orientation. Outside the EARS valley scarp the aspect of the slopes may be separately described as varying with the orientation following river valley exposition and topographic variability of the terrain, including the bathymetry of Lake Victoria. In the same manner, some subtle variations between different compass expositions in the relief of Uganda within the study area can be extended on the region between the EARS valley with Rwenzori Mountains in the SW, Lake Victoria in the S, Mount Elgon in the E and northern plains along the Achwa and Albert Nile river basins.

Figure 9 shows the hillshade visualisation map of Uganda which highlights the geomorphologic subdivision of the area into the regions based on their slope steepness and aspect highlighted using the 'cividis' colours palette for a better visibility. Hillshade closely resembles the real-world topography of Uganda that it represents, and can be self-explanatory in the absence of additional topographic data. Plotting hillshade is a standard practice by 'raster' package of R made using algorithm of computing the hillshade based on the previously made slope and aspect raster grids. The means of the artificial light source illumination of the slope consists in the computation of the

surface with artificial illumination at angle 40° and direction at angle 270°. The hillshade is employed to enable better visual recognition of the distinct relief features and gradients in Uganda.

Conclusion and future applications

The hitherto absence of a complex mapping of seismic events of Uganda in context of its tectonic, geological, geomorphologic and topographic setting was a challenge to regional thematic mapping efforts. We have developed new sets of maps, based on two cartographic tools – GMT and R – and scripting principles that may fill the current void in advanced data analysis.

Using open IRIS data with a 50-year span (1973-2021), the presented series of maps demonstrated the geomorphological variations of Uganda with a clearly notable seismicity corresponding to the geographic extension of the EARS. Application of geophysical and geomorphometric modeling and applied geological studies can also be used to estimate the agricultural potential of land in a country.

The maps of geomorphological derivatives are particularly necessary since the visualisation of the slope steepness gradient, aspect orientation (N-W-S-E) and elevations can be additional data and knowledge to analyse and assess places with better conditions for growth of plants. The presented study of scripting application for geophysical and geomorphic mapping of Uganda presents a means of estimating the geomorphic and geophysical variability of the lands with respect to the topographic setting.

Acknowledgement

This research has been implemented into the framework of the project No. 0144-2019-0011, Schmidt Institute of Physics of the Earth, Russian Academy of Sciences. IRIS Data Services are funded through the Seismological Facilities for the Advancement of Geoscience (SAGE) Award of the National Science Foundation under Cooperative Support Agreement EAR-1851048.

References

Aanyu, K. and Koehn, D. 2011. Influence of pre-existing fabrics on fault kinematics and rift geometry of interacting segments: Analogue models based on the Albertine Rift (Uganda), Western Branch-East African Rift System. *Journal of African Earth Sciences* 59(2–3): 168–184. https://doi.org/10.1016/j.jafrearsci.2010.10.003

Albuquerque Seismological Laboratory (ASL)/USGS. 1988. Global Seismograph Network (GSN – IRIS/USGS). International Federation of Digital Seismograph Networks. https://doi.org/10.7914/SN/IU

Bahiru, E.A. and Woldai, T. 2016. Integrated geological mapping approach and gold mineralization in Buhweju area, Uganda. *Ore Geology Reviews* 72(1): 777–793. https://doi.org/10.1016/j.oregeorev.2015.09.010

Batte, A.G., Rümpker, G., Lindenfeld, M. and Schumann, A. 2014. Structurally controlled seismic anisotropy above small earthquakes in crustal rocks beneath the Rwenzori region, Albertine Rift, Uganda. *Journal of African Earth Sciences* 100: 579–585. https://doi.org/10.1016/j.jafrearsci.2014.08.001

Bauer, F.U., Karl, M., Glasmacher, U.A., Nagudi, B., Schumann, A. and Mroszewski, L. 2012. The Rwenzori Mountains of western Uganda – Aspects on the evolution of their remarkable morphology within the Albertine Rift. *Journal of African Earth Sciences* 73–74: 44–56. https://doi.org/10.1016/j.jafrearsci.2012.07.001

Bauer, F.U., Glasmacher, U. A., Ring, U., Karl, M., Schumann, A. and Nagudi, B. 2013. Tracing the exhumation history of the Rwenzori Mountains, Albertine Rift, Uganda, using low- temperature thermochronology. *Tectonophysics* 599: 8–28.

Byakagaba, P., Mugagga, F. and Nnakayima, D. 2019. The socio-economic and environmental implications of oil and gas exploration: Perspectives at the micro level in the Albertine region of Uganda. *The Extractive Industries and Society* 6(2): 358–366. https://doi.org/10.1016/j.exis.2019.01.006

Calais, E., Hartnady, C., Ebinger, C. and Nocquet, J. M. 2006. Kinematics of the East African Rift from GPS and earthquake slip vector data. Geological Society, London. *Special Publications* 259: 9–22. https://doi.org/10.1144/GSL.SP.2006.259.01.03

Call, M., Mayer, T., Sellers, S., Ebanks, D., Bertalan, M., Nebie, E. and Gray, C. 2017. Socio-environmental drivers of forest change in rural Uganda. *Land Use Policy* 62: 49–58. https://doi.org/10.1016/j.landusepol.2016.12.012

Chorowicz, J. 2005. The East African rift system. *Journal of African Earth Sciences* 43(1–3): 379–410. https://doi.org/10.1016/j.jafrearsci.2005.07.019

Déprez, A., Doubre, C., Masson, F. and Ulrich, P. 2013. Seismic and aseismic deformation along the East African Rift System from a reanalysis of the GPS velocity field of Africa. *Geophysical Journal International* 193(3): 1353–1369. https://doi.org/10.1093/gji/ggt085

Ebinger, C.J. 1989. Tectonic development of the western branch of the East African rift system. *Geological Society of America Bulletin* 101: 885–903. https://doi.org/10.1130/0016-7606(1989)101<0885:TDOTWB>2.3.CO;2.

Ebinger, C. J. 2021. Recipe for rifting: Flavors of East Africa. *Encyclopedia of Geology* (2nd Edition), 271–283. https://doi.org/10.1016/B978-0-08-102908-4.00100-4

Fletcher, A. W., Abdelsalam, M. G., Emishaw, L., Atekwana, E. A., Laó Dávila, D. A. and Ismail, A. 2018. Lithospheric controls on the rifting of the Tanzanian craton at the Eyasi basin, eastern branch of the East African rift system. *Tectonics* 37: 2818–2832. https://doi.org/10.1029/2018TC005065

Guma, B.E., Owor, M. and Muwanga, A. 2019. Hydrogeological characteristics of the Albertine Graben, Uganda: Evidence from surface geophysics and hydraulic testing. *Journal of African Earth Sciences* 150: 224–238. https://doi.org/10.1016/j.jafrearsci.2018.11.008

Hijmans, R.J. and van Etten, J. 2012. raster: Geographic analysis and modeling with raster data. R package version 2.0-12. http://CRAN.R-project.org/package=raster

Herbert, S., Woldai, T., Carranza, E.J.M. and van Ruitenbeek, F.J.A. 2014. Predictive mapping of prospectivity for orogenic gold in Uganda. *Journal of African Earth Sciences* 99(2): 666-693. https://doi.org/10.1016/j.jafrearsci.2014.03.001

IRIS Transportable Array. 2003. USArray Transportable Array. International Federation of Digital Seismograph Networks. https://doi.org/10.7914/SN/TA

Kaufmann, G. and Romanov, D. 2012. Landscape evolution and glaciation of the Rwenzori Mountains, Uganda: Insights from numerical modeling. *Geomorphology* 138(1): 263–275. https://doi.org/10.1016/j.geomorph.2011.09.011

Lemenkova, P. 2020a. R Libraries {dendextend} and {magrittr} and Clustering Package scipy.cluster of Python For Modelling Diagrams of Dendrogram Trees. *Carpathian Journal of Electronic and Computer Engineering* 13(1): 5–12. https://doi.org/10.2478/cjece-2020-0002

Lemenkova, P. 2020b. Using R packages 'tmap', 'raster' and 'ggmap' for cartographic visualization: An example of dem-based terrain modelling of Italy, Apennine Peninsula. *Zbornik radova – Geografski fakultet Univerziteta u Beogradu* 68: 99–116. https://doi.org/10.5937/zrgfub2068099L

Lemenkova, P. 2020c. Variations in the bathymetry and bottom morphology of the Izu-Bonin Trench modelled by GMT. *Bulletin of Geography. Physical Geography Series* 18(1): 41–60. https://doi.org/10.2478/bgeo-2020-0004

Lemenkova, P. 2020d. Applying automatic mapping processing by GMT to bathymetric and geophysical data: Cascadia subduction zone, Pacific Ocean. *Journal of Environmental Geography* 13(3–4): 15–26. https://doi.org/10.2478/jengeo-2020-0008

Lemenkova, P. 2020e. GEBCO Gridded Bathymetric Datasets for Mapping Japan Trench Geomorphology by Means of GMT Scripting Toolset. *Geodesy and Cartography* 46(3): 98–112. https://doi.org/10.3846/gac.2020.11524

Pavlis, N.K., Holmes, S., Kenyon, S.C. and Factor, J.K. 2012. The development and evaluation of the Earth Gravitational Model 2008 (EGM2008). *Journal of Geophysical Research* 117: B04406. https://doi.org/10.1029/2011JB008916

Rooney, T. O. 2020. The Cenozoic magmatism of East Africa: Part III – Rifting of the craton. *Lithos* 360–361: 105390. https://doi.org/10.1016/j.lithos.2020.105390

Sandwell, D.T., Müller, R.D., Smith, W.H.F., Garcia, E. and Francis, R. 2014. New global marine gravity model from CryoSat-2 and Jason-1 reveals buried tectonic structure. *Science* 7346(6205): 65–67. https://doi.org/10.1126/science.1258213

Schaff, D., Shillington, D. J., Ekström, G., Nettles, M., Gaherty, J. B., Pritchard, M. E., Zheng, W., Henderson, S. T., Mdala, H., Chindandali, P. R. N., Shuler, A., Lindsey, N., Oliva, S. J., Nooner, S. and Scholz, C. A. 2019. Faulting processes during early-stage rifting: Seismic and geodetic analysis of the 2009–2010 Northern Malawi earthquake sequence. *Geophysical Journal International* 217(3): 1767–1782. https://doi.org/10.1093/gji/ggz119

Schenke, H. 2016. General Bathymetric Chart of the Oceans (GEBCO). In: Harff J., Meschede M., Petersen S., Thiede J. (eds.) Encyclopedia of Marine Geosciences. Encyclopedia of Earth Sciences Series. Springer, Dordrecht. https://doi.org/10.1007/978-94-007-6238-1_63

Schneider, S., Hornung, J. and Hinderer, M. 2016. Evolution of the western East African Rift System reflected in provenance changes of Miocene to Pleistocene synrift sediments (Albertine Rift, Uganda). *Sedimentary Geology* 343: 190–205. https://doi.org/10.1016/j.sedgeo.2016.07.013

Simon, B., Guillocheau, F., Robin, C., Dauteuil, O., Nalpas, T., Pickford, M., Senut, B., Lays, P., Bourges, P. and Bez, M. 2017. Deformation and sedimentary evolution of the Lake Albert Rift (Uganda, East African Rift System). *Marine and Petroleum Geology* 86: 17–37. https://doi.org/10.1016/j.marpetgeo.2017.05.006

Tennekes, M. 2012. tmap: Thematic Maps in R. *Journal of Statistical Software* 84(6): 1–39.

Xue, L., Johnson, C. W., Fu, Y. and Bürgmann, R. 2020. Seasonal seismicity in the western branch of the East African Rift System. *Geophysical Research Letters* 47: e2019GL085882. https://doi.org/10.1029/2019GL085882

Wessel, P., Luis, J.F., Uieda, L., Scharroo, R., Wobbe, F., Smith, W.H.F. and Tian, D. 2019. The Generic Mapping Tools version 6. *Geochemistry, Geophysics, Geosystems* 20: 5556–5564. https://doi.org/10.1029/2019GC008515